Vibrational spectroscopic study on the quantum chemical model and the X-ray structure of gallic acid, solvent effect on the structure and spectra

ARTICLE *in* VIBRATIONAL SPECTROSCOPY · JANUARY 2007

Impact Factor: 2 · DOI: 10.1016/j.vibspec.2006.07.008

3 AUTHORS:

Ferenc Billes
Budapest University of Technology and Eco…
67 PUBLICATIONS **841** CITATIONS
SEE PROFILE

Ildikó Ziegler (formerly Mohammed-Ziegler)
Gedeon Richter Plc
38 PUBLICATIONS **389** CITATIONS
SEE PROFILE

P. Bombicz
Hungarian Academy of Sciences
104 PUBLICATIONS **912** CITATIONS
SEE PROFILE

Available online at www.sciencedirect.com
ScienceDirect
Vibrational Spectroscopy 43 (2007) 193–202
VIBRATIONAL SPECTROSCOPY
www.elsevier.com/locate/vibspec

Vibrational spectroscopic study on the quantum chemical model and the X-ray structure of gallic acid, solvent effect on the structure and spectra

Ferenc Billes [a,*], Ildikó Mohammed-Ziegler [b,1], Petra Bombicz [c]

[a] Department of Physical Chemistry, Budapest University of Technology and Economics, H-1521 Budapest, Budafoki út 8, Hungary
[b] H-2521 Csolnok, Arany J. u. 28, Hungary
[c] Institute of Structural Chemistry, Chemical Research Center, Hungarian Academy of Sciences, H-1025 Budapest, Pusztaszeri út 59-67, Hungary

Received 27 April 2006; received in revised form 5 July 2006; accepted 7 July 2006
Available online 28 August 2006

Abstract

Infrared, Raman and far-IR spectra of gallic acid were recorded both in crystalline and in its dry form. Solvent effect of water was studied. The molecular and crystal structures were determined by single crystal X-ray diffraction. A complex system of intermolecular interactions was revealed. Optimized geometries, vibrational frequencies and infrared intensities were calculated utilizing the post-HF DFT method with the Becke3LYP functional and the 6-31G* basis set. Normal coordinate analysis was carried out. The results of the calculations were applied to simulate the infrared and Raman spectra and the full assignment of the acquired spectra is presented.

Keywords: Vibrational spectra; Quantum chemistry; Single crystal X-ray diffraction; Gallic acid; Solvent effect

1. Introduction

Gallic acid (3,4,5-trihydroxybenzoic acid, Fig. 1) is one of the most well-known extractive components of plants. It can be isolated, for instance, from some hardwood species such as oak trees (e.g. *Quercus robur*, *Q. alba*, *Q. rubra*), chestnut (*Castanea sativa* L.) and many others [1–10], grape, different berries, fruits as well as wine [11–17]. Gallic acid and its derivatives exhibit biological activity, their antioxidant and anticancer effect arosed the interest of many scientists, and they are also known to display fungicidal/fungistatic properties [1–7,11–13,18]. Moreover, they tend to form complexes with metal ions, thus they are used for analytical purposes [19–22]. Due to these versatile features, numerous results were reported on the theoretical studies of gallic acid and other phenol type compounds [23–31] in some of which structural characteristics of these compounds were correlated to their biological activity. An excellent theoretical investigation of the possible conformers of gallic acid is presented by Capelli et al. [32].

As Ribeiro-Claro and Amado emphasized in their comment [33], embedded water molecules in the molecular structure of any solid alters the vibrational spectra significantly in comparison with those of the dry solid.

The aim of this work was the interpretation of the vibrational spectra of crystalline gallic acid based on the single crystal X-ray structure. In the present paper, the full assignment of the infrared, Raman and far-IR spectra is aimed by means of DFT calculations and the normal coordinate analysis. Moreover, the spectral changes due to the presence of water in the crystal structure and the solvent effect of water are analysed. The quantum chemical model was constructed from a water molecule between two gallic acid molecules, GWG (see Fig. 6).

2. Experimental

2.1. Materials

Gallic acid was purchased from Merck (99.5%) and used without any further purification. For the single crystal X-ray

* Corresponding author. Tel.: +36 1 463 1267; fax: +36 1 463 3767.
E-mail addresses: fbilles@mail.bme.hu (F. Billes), mohazihu@yahoo.com (I. Mohammed-Ziegler), bombicz@chemres.hu (P. Bombicz).
[1] Present address: Gedeon Richter Ltd., Quality Control Department, Analytical Laboratory, Esztergomi út 27, H-2510 Dorog, Hungary.

0924-2031/$ – see front matter © 2006 Elsevier B.V. All rights reserved.
doi:10.1016/j.vibspec.2006.07.008

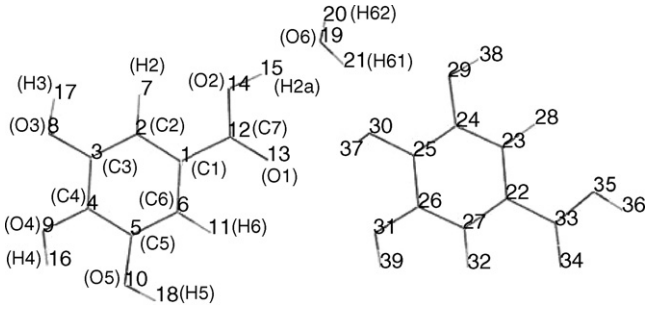

Fig. 1. Numbering of the atoms in quantum chemical results and their corresponding labeling in X-ray diffraction data (in brackets).

diffraction experiment, it was re-crystallized from 50 vol.% aq. ethanol. Ethanol was the product of Merck (96%, extra pure).

2.2. Single crystal X-ray diffraction

A light yellow, needle shape single crystal of the size 0.60 mm × 0.07 mm × 0.05 mm of gallic acid ($C_7H_8O_6$, F_w: 188.13, $F(0\,0\,0) = 392$) was mounted on a glass fiber. Cell parameters were determined by least-squares of the setting angles of 25 ($30.35^\circ \leq \theta \leq 39.60^\circ$) reflections: $a = 14.158$ (3) Å, $b = 3.624$ (1) Å, $c = 15.036$ (3) Å, $\beta = 97.60$ (3)°, $V = 764.7$ (3) Å^3. The calculated density is $\rho = 1.634$ Mg m^{-3}. 3. The gallic acid crystallizes in monoclinic crystal system and $P2/n$ space group (13), $Z = 4$. Intensity data were collected on an Enraf-Nonius CAD4 diffractometer (graphite monochromator; Cu Kα radiation, λ = 1.54184 Å) at 293 (2) K in the range $1.86^\circ \leq \theta \leq 26.50^\circ$ using ω–2θ scans. The scan width was 0.111° in ω. Backgrounds were measured for half of the total time of the peak scans. The intensities of three standard reflections were monitored regularly in every 60 min. They indicated a crystal decay of 2%, therefore the data were corrected for decay. Data reduction was carried out by XCAD4 [34]. A total of 1720 reflections were collected of which 1587 were unique [R(int) = 0.0100, $R(\sigma) = 0.0210$]; 1249 reflections were stronger than $2\sigma(I)$. Completeness to 2θ is 0.996. Semi empirical ψ-scan absorption correction was applied, $\mu = 0.147$ mm^{-1}, maximum and minimum transmissions are 0.9927 and 0.9171.

The structure was solved by direct methods [35]. Anisotropic full-matrix least-squares refinement [36] on F^2 for all non-hydrogen atoms yielded $R_1 = 0.0534$ and $wR_2 = 0.1627$ for 1249 [$I > 2\sigma(I)$] and $R_1 = 0.0657$ and $wR_2 = 0.1725$ for all (1587) intensity data, goodness-of-fit is 1.082; the maximum and mean shift/esd are 0.002 and 0.000; the extinction coefficient is 0.062 (13). The extinction coefficient expression: $F_c^* = kF_c[1 + 0.001F_c^2\lambda^3/\sin(2\theta)]^{-1/4}$. Number of parameters is 124. The maximum and minimum residual electron density in the final difference map was 0.500 and −0.308 e/Å^3. The weighting scheme applied was: $\omega = 1/[\sigma^2(F_o^2) + (0.1257P)^2 + 0.0471P]$, where $P = (F_o^2 + 2F_c^2)/3$. Neutral atomic scattering factors are taken from the International Tables for X-ray Crystallography [37].

Hydrogen atomic positions were located in difference maps. Hydrogen atoms were included in structure factor calculations but they were not refined. The isotropic displacement parameters of the hydrogen atoms were refined. The deposited material contains further details.

2.3. Vibrational spectroscopic measurements

Diffuse reflectance infrared Fourier transform spectra (DRIFTS) of the dry and the polycrystalline compound were measured in KBr matrix on a Perkin-Elmer System 2000 FT-IR spectrometer at a 1 cm^{-1} resolution accumulating 512 scans. DRIFTS technique was chosen because of the expected application of these data. Gallic acid as a fungicidal compound is a promising wood preservative. The IR spectra of wood samples can be observed most conveniently in the form of sawdust by the DRIFTS method using the FT-IR techniques.

Raman spectra were recorded on a Perkin-Elmer System 1760× FT-IR spectrometer equipped with a 1700× Raman accessory. Eight-hundred and fifty scans were accumulated at a resolution of 1 cm^{-1}. The sample was excited with 0.8 W (for gallic acid) power from a Spectron SL 301 Series Nd:YAG laser intensity stabilized at 1064 nm. The Raman spectrum of the saturated (at 22 °C temperature) aqueous solution of gallic acid and the neat solvent were recorded on a Bio-Rad FT-Raman spectrometer using liquid nitrogen cooled Ge detector and excited by a Spectra-Physics Nd:YAG laser at its 1064 nm line with 3 W power. In this experiment 1064 scans were collected.

3. Computational details

Quantum chemical calculations were carried out by means of the Gaussian 03 program package with the Becke3LYP DFT functional and the 6-31G* basis set [38]. Although Capelli et al. [32] proposed to use larger basis set, the presented results in this paper suggest that the 6-31G* basis set is sufficient for the exploration of the effect of crystalline structure.

The full geometry optimizations were carried out by minimization of the molecular energies. The conformation of the molecule at optimized geometries of the studied molecules is presented in Fig. 6. This geometry is identical with that used in our previous paper [27]. Since the possible number of rotations is five in the molecule of gallic acid, it would mean a serious difficulty to carry out a full conformational analysis for the structure of crystalline gallic acid, i.e. the GWG system. Our main goal is to construct a simpified model of the solid gallic acid determined by X-ray measurements in order to observe the gallic acid–crystalline water interactions whereas Capelli et al. [32] delt with a theoretical model in gaseous and liquid state. The starting point of our simulation corresponding to aqueous media is also the crystalline structure, i.e. in the present study the effect of water on the gallic acid crystal structure is observed.

The numbering of the atoms in Fig. 1 refers both to the quantum chemical calculations and the X-ray crystallographic measurement.

In the next step, the force constants were calculated by differentiating the molecular potential energy twice with

respect to the Cartesian coordinates of the atoms. The harmonic vibrational frequencies and IR intensities were calculated, too.

The calculated geometry and the force field were applied to the further force field refinement in internal coordinate representation by means of a set of scaling factors to fit the calculated frequencies to the experimental ones. At first approximation, the scaling factors were chosen being identical with those applied for phenol [23] and gallic acid [27]. The potential energy distribution (PED) matrix elements were calculated with this scaled force field. The normal coordinate calculations and the calculations for the simulated spectra were carried out with our home-made computer programs.

Simulated vibrational spectra are based on the scaled vibrational frequencies and the quantum chemically resulted infrared and Raman intensities. Lorentz type bands were applied with 15 cm^{-1} FWHH.

4. Results and discussion

4.1. Single crystal X-ray diffraction

The crystal structure of 3,4,5-trihydroxybenzoic acid monohydrate has two known polymorphs: it crystallizes in the space groups $P2_1/c$ [39] and $P2/n$ [40]. The aim of this study is to discuss the rather complex hydrogen bond system in crystal $P2/n$ in details. The gallic acid molecule is highly planar. It explains the fact that its crystal structure was not known until recently because of the difficulties of growing single crystal. The ORTEP [41] representation of molecular structure of 3,4,5-trihydroxybenzoic acid in $P2/n$ is shown in Fig. 2. The b axis of the unit cell is very short 3.624 (1) Å, while a and c axes are about four times longer.

In the Cambridge Structural Database [42] there are now over 355,000 entries of organic and organometallic crystal structures. The shorter the cell axis is, the exponentially less is the number of structures. There are 2739 crystals in which one of the crystal axes is shorter than 4 Å, and 296 structures with a shorter axis than 3.6 Å.

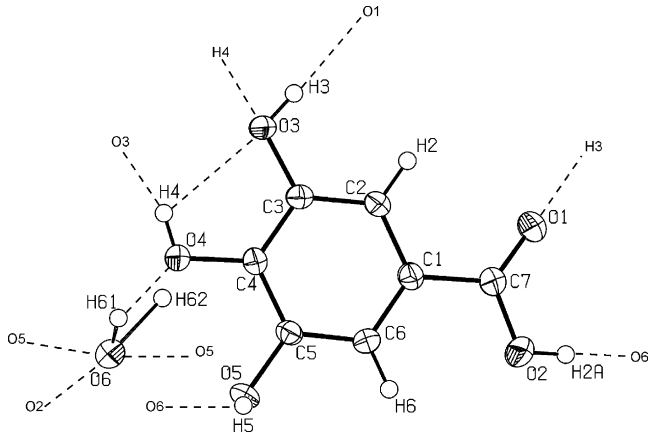

Fig. 2. Structure of gallic acid and the atom labels for the X-ray crystallographic study.

Table 1
Distances from the plane defined by the carbon atoms in the gallic acid molecule

Name of atom	Distance from the plane (Å)
C1*	0.027 (2)
C2*	0.041 (2)
C3*	−0.012 (2)
C4*	−0.035 (2)
C5*	0.002 (2)
C6*	0.025 (2)
C7*	−0.048 (2)
O1	−0.112 (2)
O2	−0.077 (2)
H2A	−0.231 (2)
O3	−0.071 (2)
H3	−0.016 (2)
O4	−0.102 (2)
H4	−0.062 (2)
O5	−0.028 (2)
H5	0.739 (2)

The equation of the plane is formed by the carbon atoms by fractional and orthogonal coordinates:

$$5.01\,(1)x + 3.394\,(1)y - 0.37\,(1)z = 0.474\,(5),$$

$$0.3500\,(7)\mathrm{XO} + 0.9364\,(3)\mathrm{YO} - 0.0250\,(7)\mathrm{ZO} = 0.474\,(5).$$

All of the atoms of the molecule are approximately in the plane (Fig. 2 and Table 1) except H5 hydrogen atom, what is placed perpendicular to it, C6–C5–O5–H5 torsion angle is 90.10°. This H5 atom connects the layers of the gallic acid molecules in the crystal *via* the water of crystallization.

Packing of the molecules in the crystal viewed down the crystallographic b and c axes, respectively, are shown in Fig. 3. Hydrogen atoms are omitted for clarity. The highlighted column in the diagonal of the a and c axes is organized by O–H···O type intermolecular interactions of the molecules (Table 2, Fig. P3, deposited). The molecules are in antiparallel arrangement in the column.

The hydrogen bond system is rather complex (see the deposited Fig. P3): all six oxygen atoms and all hydrogen atoms except the aryl ones are taking part in strong O–H···O type hydrogen bonds. Two of the hydrogens are bifurcated: H4 and H62. H4 takes part in an intra- and an intermolecular interaction. There is one intramolecular hydrogen bond in the molecule.

The graph-set analysis of hydrogen bond pattern [43] reveals four hydrogen bonded rings in the crystal (Fig. 4). The designator denotes the number of hydrogen bond acceptors in superscript, donored hydrogens in subscript, and the smallest number of atoms required to define the pattern in parentheses. One of the rings $R_2^2(4)$ is organized by the two-fold axis and by hydrogen bonds signed 3 and 4. The biggest ring $R_4^4(10)$ is homodromic and consists of hydrogen bonds number 1, 2, 4 and 6. There is a smaller ring in contact with the previous one, which is $R_2^2(7)$ by hydrogen bonds number 5 and 6. The fourth ring of hydrogen bonds $R_2^2(4)$ consists of the out of plane H5

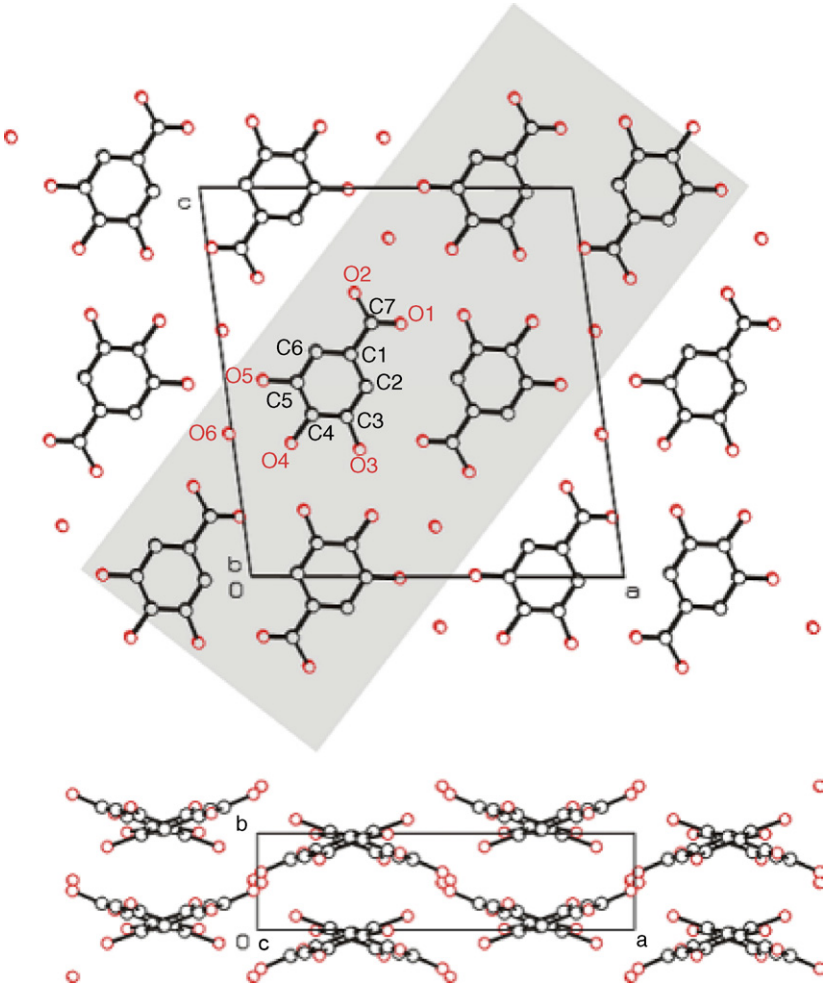

Fig. 3. Crystal packing of gallic acid viewed from the *b* and *c* crystallographic axes, respectively.

hydrogen of gallic acid and the oxygen of the water molecule (hydrogen bond marked 5) repeated by the symmetry center thus connecting the columns to each other (Fig. 5).

The water molecules join the layers of the gallic acid. One water molecule connects to four gallic acid molecules by hydrogen bonds (Fig. 5). The water oxygen is acceptor of three hydrogen atoms. The water hydrogens are donors to three gallic acids oxygens, *viz.* one of the water hydrogens (H62) is bifurcated to the O4 and O5 oxygen of the same gallic acid molecule. In accordance of the strong hydrogen bonds of the water molecule it occupies a relatively small volume of 28.5 Å per molecule in the unit cell.

4.2. Structure of the GWG system

As it was already mentioned a simplified model was constructed for crystalline gallic acid. Of course, this model contains most of the possible intermolecular interactions and hydrogen bond types existing in the crystal but if considering the possibilities of the quantum chemical calculations, not all.

Table 2
Intermolecular interactions in the crystal structure of gallic acid

Number	Donor-H···accept.	Symm. code	D–H	H···A	D···A	D–H···A
1	O2–H2A···O6	$1/2 - x, -1 + y, 3/2 - z$	0.8652	1.8258	2.688 (2)	173.86
2	O3–H3···O1	$1 - x, -1 - y, 1 - z$	0.8195	1.9196	2.723 (2)	166.27
3	O4–H4···O3	Intra	0.8201	2.3355	2.762 (2)	113.04
4	O4–H4···O3	$1/2 - x, y, 1/2 - z$	0.8201	2.0433	2.765 (2)	146.57
5	O5–H5···O6	$-x, 1 - y, 1 - z$	0.8199	2.4575	2.764 (2)	103.31
6	O6–H61···O4	$-x, -y, 1 - z$	0.8961	2.1289	2.977 (2)	157.64
7	O6–H62···O4	$-x, 1 - y, 1 - z$	1.4054	1.7843	3.073 (2)	148.65
8	O6–H62···O5	$-x, 1 - y, 1 - z$	1.4054	2.0006	2.764 (2)	107.19

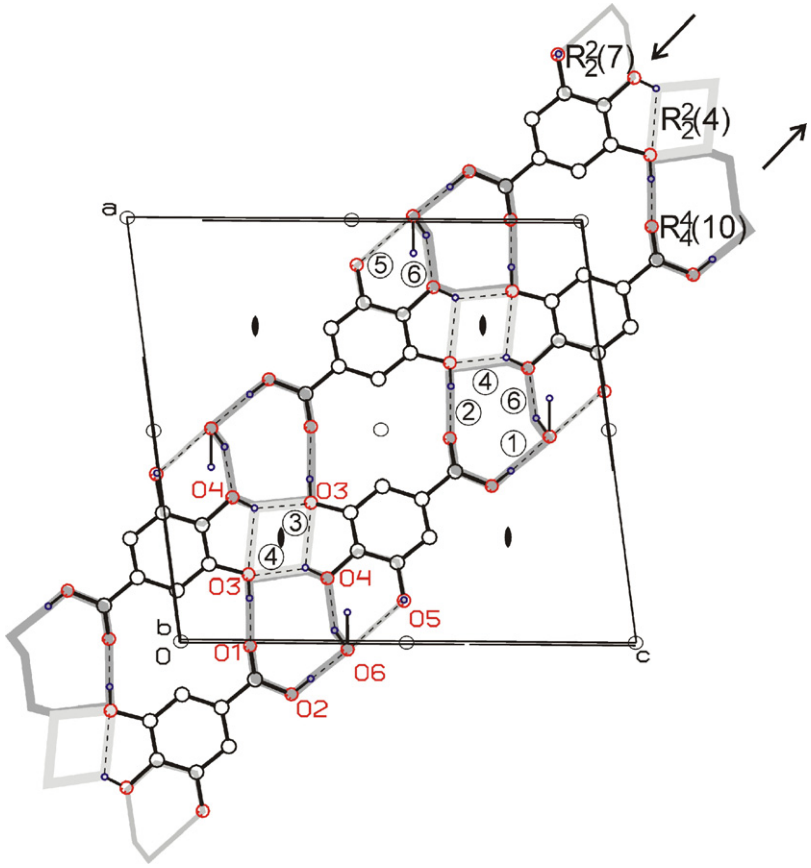

Fig. 4. The column of the molecules in the diagonal of the *a* and *c* directions in the unit cell organized by intermolecular interactions. Crystallographic symmetry elements of the *P*2/*n* cell: two-fold axes and symmetry centers are indicated.

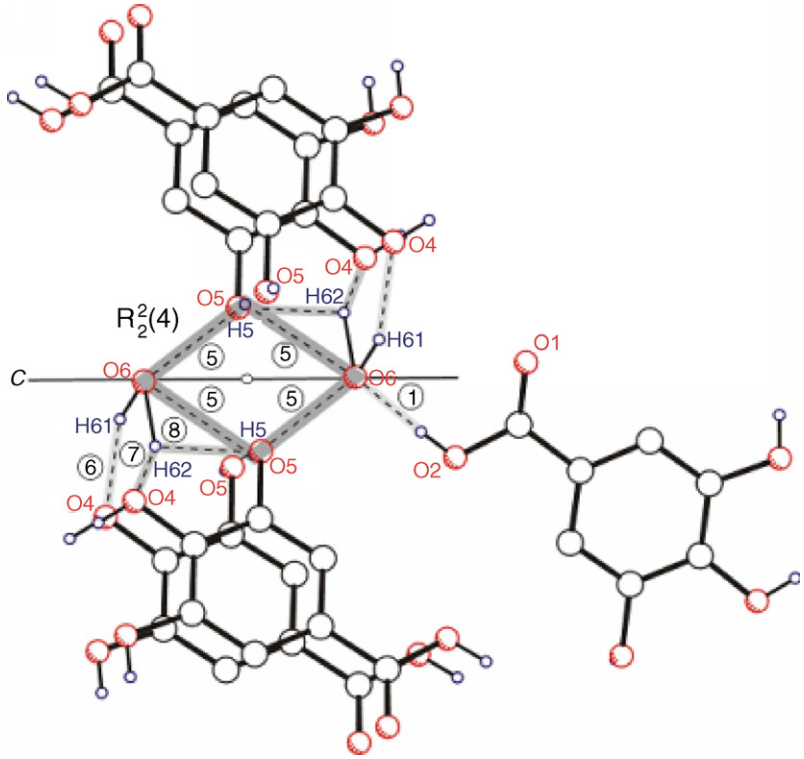

Fig. 5. Intermolecular interactions between the columns. Oxygen atoms are shaded. Aromatic hydrogens are omitted for clarity. The direction of the *c* crystallographic axis and the symmetry center are marked.

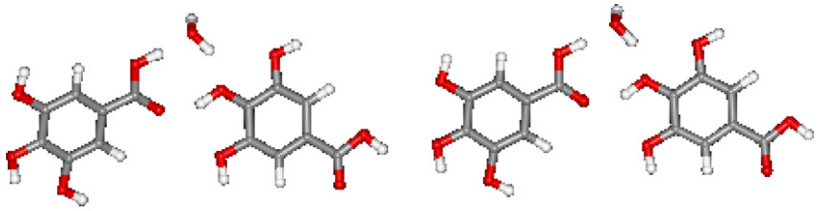

Fig. 6. Optimized structures of GWG.

Fig. 6 presents the optimized structures of isolated GWG and that in aqueous solution according to the Onsager's dipole field model [44]. The difference is minor.

Due to the characteristic differences between X-ray diffraction and quantum chemical calculations, different numbering of the atoms was necessary to apply (see Fig. 1).

Experimental and calculated optimized parameters are shown in Table 3 of the supplementary material. Comparing the results, the quantum chemical entries show the effect of water on gallic acid in two steps: effect of the water molecule as water of crystallization and that of the dipole field. The parameters of the isolated molecule changes in GWG, above all, for the carboxylic group. The bond distances C1–C12, C12–O13, C14–C15 increase with some hundred ångstroms, while the C12–O14 distance shortens, i.e. the difference between the C–O and the C=O bonds decreases. Changes are observable for valence angles and dihedral angles connected to the carboxylic group. Certainly, the interaction between two gallic acid and the water molecules are not symmetric, e.g. the bond length O30–H37 is longer than the corresponding O8–H17 one (for details see the deposited Table 3). The quantum chemical results show hydrogen bonds between O13 and H37, C15 and H19, C21 and C30. The first of them is between the two gallic acid molecules, while the two others are connected to the water molecule, i.e. every three molecules are connected to one another *via* hydrogen bonds. These results are in agreement with the findings of the X-ray structural study (see Table 2).

The solvent acting like dipole field in the quantum chemical calculations has smaller effect on the GWG geometry. While the gallic acid structures show only minor changes, changes are significant in the hydrogen bond lengths: the increased O13–H37 distance and the decreasing O15–H19 and O30–H21 ones reflect the moving away the two gallic acid molecules from one another and the same time their nearing to the water molecule.

The chemical environment for the quantum chemically calculated structures (isolation or dipole field) differ substantially from that of the gallic acid in the crystal. Besides, every quantum chemical method is an approximation. These factors are major reasons for the deviation between calculated structure and that obtained by X-ray crystallography. The C–C distances in the X-ray results are some hundred ångstroms shorter than the GWG distances. Similarly, the C–O distances in the carboxylic group are shorter, while these kinds of distances in C–OH structures are longer than the quantum chemically calculated ones (see e.g. C3–O8 distance).

4.3. Atomic net charges

The changes in the chemical environment are reflected also in the shifts of atomic net charges. The natural atomic net charges, results of the NBO/NPA calculations, are listed in Table 4 (deposited).

The distribution of the natural atomic net charges of the aromatic ring of the isolated gallic acid (column ''without interaction'', atoms 1–6 and 22–27, respectively) reflects the effects of the four substituents on the benzene ring.

The difference between the two gallic acid molecules in GWG (see Fig. 1) is also exhibited in the charge distribution. The positions of the two gallic acid molecules to the water molecules are very different, therefore the results of the interactions are also different.

In the ring of the left side gallic acid molecule (LSGA, see Fig. 1) atoms C1, C2, C3 and C4 become more positive, while C5 becomes more negative. In the carboxylic group drastic changes are found in the net charge of C13, where the shift to negative direction is more than 0.1 atomic charge units. Here, the charges of H15 and C12 shift to the positive, O14 to the negative direction. Summarizing up, all bonds of the carboxylic group becomes more polarised. These changes are also reflected in the alteration of the bond lengths inside the carboxylic group (see Table 4). It is interesting that the effects on the oxygen atoms of the hydroxyl groups are very different. Strong effects are found on those OH oxygen atoms that are situated in meta position to the carboxylic group (O8 positive shift, O10 negative shift), while the charge of O10 remained practically constant.

The effect of the intermolecular hydrogen bond on the other gallic acid molecule (RSGA, on the right side of Fig. 1) is different. The net charges of the carbon atoms C23 and C24 show positive, while that of the C26 shows negative shift. Comparing the behaviour of the carboxylic group atoms O34 and O35, they become more negative, atom H36 shows positive shift, while the charge of C33 remains practically constant. Regarding the OH groups of this molecule, the O30–H37 group being in hydrogen bond with the water molecule shows a strong polarisation effect. The charges of the other OH oxygens show opposite shifts, positive for O29 and negative for O31.

The presence of hydrogen bonds has effect also on the water molecule of GWG. The asymmetry of the molecule is exhibited not only in the structure (Table 3) but also in the charge distribution. The strongest effect can be observed on atoms O19 and H21 since they are in strong interactions with the gallic acid molecules.

The effect of Onsager's dipole field is essentially less remarkable than that of the water molecule.

4.4. Vibrational force constants

Values of the diagonal vibrational force constants of GWG are presented in Table 5 (deposited) together with the definition of the applied internal coordinates and the used scale factors. Since GWG consists of 39 atoms, 111 independent internal coordinates describe its vibrational motion. The scaling to the measured fundamental frequencies was performed using the vibrational spectra of the crystalline gallic acid. The same scale factors were also used for the scaling of the yielded force constants of dipole field (solvent effect) calculations.

The majority of the scale factor values are in the range of 0.9–0.95. Smaller scale factors, e.g. those belonging to the carboxylic groups, reflect the effect of the strong intra- and intermolecular interactions and are between 0.7 and 0.9. The intermolecular interactions are the reasons of the high scale factor values of the OH stretch modes of water.

The inequality of the two gallic acid molecules was already mentioned in the discussion of the geometric parameters and the atomic net charges (see above), as it is also apparent from the values of obtained vibrational force constants.

4.5. Vibrational frequencies and fundamental modes

The experimental fundamental vibrational frequencies of the crystalline gallic acid were compared with the calculated ones of GWG. Their values with the calculated potential energy distributions are shown in Table 6 of the supplementary material.

Above all we pay attention to the high frequency part (over 2500 cm^{-1}) of Table 6. Fourteen fundamental frequencies are found in this region. GWG contains 10 OH groups and 4 CH ones. The following OH stretch coordinates were defined: six phenolic ones, two of them in COOH groups, two belonging to the water molecule and two along intermolecular hydrogen bonds (see Table 5 (deposited) and Fig. 1). One of the water OH stretches has the highest frequency and is characteristic, while the other one is distributed in several other vibrational modes. The two OH stretch coordinates of the COOH groups have very different characteristic frequencies: this frequency of the RSGA molecule (see Fig. 2) is 3458 cm^{-1}, that of the other one on the left side is centered at 2868 cm^{-1} frequency, reflecting the very strong intermolecular interaction H15–O19.

The three OHh stretch coordinates of LSGA (see Fig. 2) build characteristic vibrational modes with frequencies at 3432, 3413 and 3371 cm^{-1}, respectively. The lowest one belongs to the OH group in para position to the COOH moiety.

The movements of some OH stretch type internal coordinates are mixed in the vibrational modes with frequencies at 3424, 3423 and 3411 cm^{-1}. The internal coordinate of the O30–H21 hydrogen bond participates in all three vibrational modes. The two stretch coordinates of the water molecule cover only a small part of potential energy of the first and third mentioned modes, the rest of its energy is distributed under several vibrational modes. The coordinates mentioned as OHh in these modes belong to RSGA, namely to O29–H38 and O31–H39. Similarly, the stretch coordinate H15–O19 does not exhibit characteristic vibrational modes. The third OHh coordinate of RSGA, O30–H37, characterizes a vibrational mode; however its characteristic frequency shifted at least by 300 cm^{-1} to lower frequencies in comparison with the location of all other similar modes. The reason is, likely, the very strong intermolecular interaction, the hydrogen bonds O13–O37 and O30–H21.

The four CH stretch coordinates exhibit characteristic vibrational modes with frequencies in a very narrow region.

One can regard the vibrational bands at the 1695 and 1635 cm^{-1}, respectively as vibrational modes characterized by C=O stretch coordinates of the carboxylic groups. The different interactions of the two COOH groups do appear here. Namely, the C12=O13 group of LSGA is in very strong intermolecular interaction (1635 cm^{-1}), while the other one is not (1695 cm^{-1}).

All other internal coordinates are distributed between lots of vibrational modes and cannot be regarded as bases of characteristic vibrational modes. The order of the two vibrations dominated by C=O stretch motions is almost unchanged, only minor frequency shifts can be found. However, the lower frequency of the C12–O13 stretch mode in comparison to the higher one C33–O34 stretch mode reflect the difference in the polarity of the two bonds (see Table 4), i.e. the different intermolecular interactions of the two carboxylic groups.

The vibrational spectra of GWG in aqueous environment are calculated using the same scale factors as for the isolated GWG for the scaling of its quantum chemically computed force constants. Doing so, the changes in the calculated values are more striking. The most characteristic frequencies and the corresponding PED elements are shown in Table 7 (deposited).

Already at first glance one can establish a rearrangement of the calculated OH valence vibrations in comparison to those of the isolated GWG. As long as the isolated GWG is considered, only three OHh groups exhibit characteristic vibrational modes, whereas one can find five such kind ones when GWG is surrounded by water as solvent. The O30–H37 stretch participates in three fundamentals, namely in those located at 3117, 3115 and 3113 cm^{-1}, respectively. It is interesting that in these modes they are mixed with CH stretch coordinates as partners. These are the C32–H28 stretch (the two higher frequencies) and the C2–H7 one. The O30–H19 intermolecular OHi stretch coordinate plays important role only in the fundamental at 3395 cm^{-1} frequency important role where its partner is the O19–H21 OHw type stretch. Similarly, minor frequency shifts are computed for the characteristic CH and OHh vibrations. As it was mentioned above, the C23–H28 coordinate takes part in two fundamentals. The order of the two vibrations dominated by C=O stretch motions is unchanged, only minor frequency shifts can be found.

The fundamental frequencies and PED of isolated gallic acid were recalculated [27] with B3LYP/6-31G* and rescaled to the experimental vibrational spectra of dry gallic acid, making it in this way comparable to the computed GWG entries. The

deposited Table 8 contains these measured and calculated fundamentals and the PE distributions.

Investigating the shifts of the group frequencies during the transition from the isolated gallic acid molecule to the GWG system some striking changes can be observed (see Tables 6 and 7, both are deposited).

Beside the simple comparison of the fundamentals we tried to explain the reason of the frequency shifts. Therefore we compare also the corresponding bond lengths (Table 3) and the net charges of the head atoms of the bonds (Table 4).

The LSGA molecule in GWG interacts with the water molecule through its carboxylic group, while RSGA does it through its middle hydroxylic group. These different interactions are reflected in the different values of the corresponding group fundamental frequencies. The changes in the group frequencies of the polar groups are very interesting.

Two fundamentals characterize the carboxylic groups: νOHk and νC=Ok. The net charge difference in LSGA OHk bond increases 0.068 a.u. and the bond length stretched with 0.038 Å. The same effects in RSGA are only 0.025 a.u. and 0.004 Å, respectively. It is discernible from the data that the low frequenccy shifts of OHk frequencies are greater for LSGA than for RSGA. Indeed, the calculated LSGA νOHk frequency shifted from 3538 to 2880 cm^{-1}, while the same for RSGA show a smaller shift to 3458 cm^{-1}. For the C=Ok bond of LSGA the net charge difference increases by 0.092 a.u., the bond length increases by 0.024 Å, for the corresponding data for RSGA are 0.042 a.u. and 0.008 Å. The calculated frequencies reflect these results. The 1714 cm^{-1} νC=Ok frequency of gallic acid shifts −79 cm^{-1} for LSGA and only −19 cm^{-1} for RSGA.

Gallic acid molecules have three OH groups. Of course, their group frequencies shift also under the effect of the interactions of LSGA and RSGA with the water molecule in GWG. The behaviour of the members of the O9–H16 and O30–H37 bond pair is very different since O30 participates in a strong hydrogen bond interaction. The net charge difference of O9–H16 (LSGA) shifts −0.002 a.u., the O–H distance does not change, while for O30–H37 (RSGA) these data are 0.138 a.u. and 0.019 Å. In accordance with these data the 3420 cm^{-1} OH stretch frequency of gallic acid decreases only by 49 cm^{-1} (LSGA) but by 350 cm^{-1} for O30–H37 (RSGA). The second bond pair is O8–H17 (LSGA) and O29–H38 (RSGA). The changes for O8–H17 are 0.054 a.u. and 0.001 Å, and 0.040 a.u. and 0.001 Å for O29–H38. The corresponding 3480 cm^{-1} νO8–H17 frequency of gallic acid shifted to 3413 cm^{-1} (LSGA) and 3423 cm^{-1} (common mode with O31–H39, RSGA). The third bond pair is O10–H18 (LSGA) and O31–H39 (RSGA). The net charge difference shift of O10–H18 is 0.059 a.u., the bond length decreases by 0.001 Å, while the similar data for O31–H39 are 0.025 a.u. and the bond length decreases also by 0.001 Å. In this case the 3458 cm^{-1} νO10–H18 frequency of gallic acid decreased by 26 cm^{-1} for νO10–H18, and by 35 cm^{-1} for νO31–H39 (common mode with O29–H38). The frequency shifts of the last two vibrational mode pairs show clearly the important role of the change in the bond polarisation, namely here the changes in the bond distances are negligible, only the shifts in the net charge differences are significant.

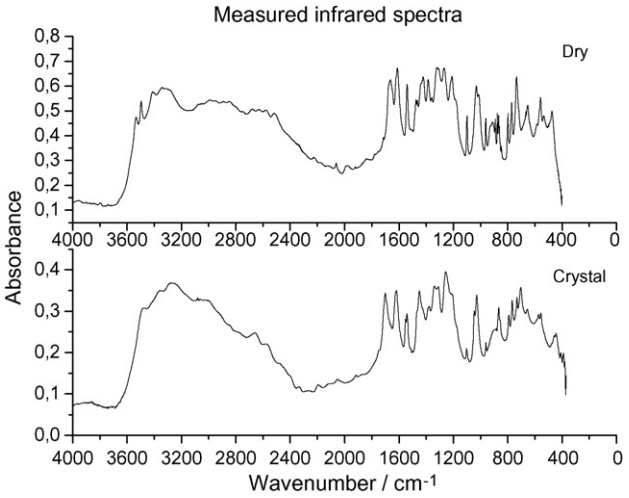

Fig. 7. Measured infrared spectra of gallic acid.

4.6. Experimental and simulated spectra

The measured infrared spectra of dry gallic acid and the crystalline gallic acid are shown in Fig. 7. The most striking difference between the two spectra is the disappearance of the 3495 cm^{-1} band in the crystal spectrum characterizing the isolated OH stretch vibration mode. Some other bands changed their intensities or shifted.

Fig. 8 contains the simulated infrared spectra of the isolated gallic acid, of GWG and the GWG in dipole field. The quantum chemically calculated band intensities not always correlate with the experimental ones. The reason is, probably, the applied intensity model. Besides, uniform FWHH values are used. Therefore the intense bands are high and narrow. However, by this method, it is easy to study the effect of water of crystallization and the water media as solvent (two different effects) acting on the isolated gallic acid molecule. The added water molecule (i.e. the water of crystallization) had very strong effect on gallic acid by increasing the number of the intermolecular hydrogen bonds significantly. This fact is

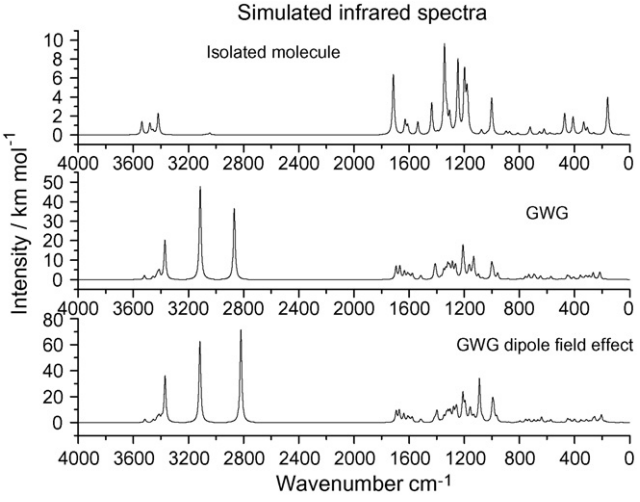

Fig. 8. Simulated infrared spectra of gallic acid.

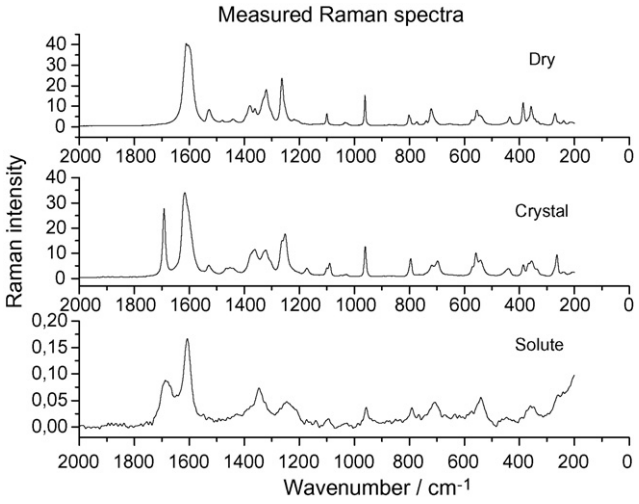

Fig. 9. Measured Raman spectra of gallic acid.

reflected in the major low frequency shifts of the OH stretch bands, e.g. the O14–H15 band (see also Tables 6 and 8).

The measured Raman spectra of gallic acid are shown in Fig. 9. Since the intensity of the OH stretch bands is very low in Raman spectra, we omitted this part of the spectra in the figure. The solute spectrum is the difference of the saturated aqueous solution of gallic acid spectrum and that of the solvent, and therefore the obtained spectrum is noisy and not very intense. Thus, the number of observed bands is essentially less than that in the other spectra. A new band appears on the effect of the water molecule belonging to the shifted and intensified C33═O34 stretch mode. Some bands are broader in the crystal spectrum than in that of the dry compound. It also has to be noted that the Raman intensities are calculated based on the static approximation, therefore the comparison of the simulated and measured spectra allow only carefully drown conclusions.

The higher frequency part of the simulated Raman spectra (Fig. 10) is more intense than that of the measured ones. Therefore the full spectra are presented. The applied quantum

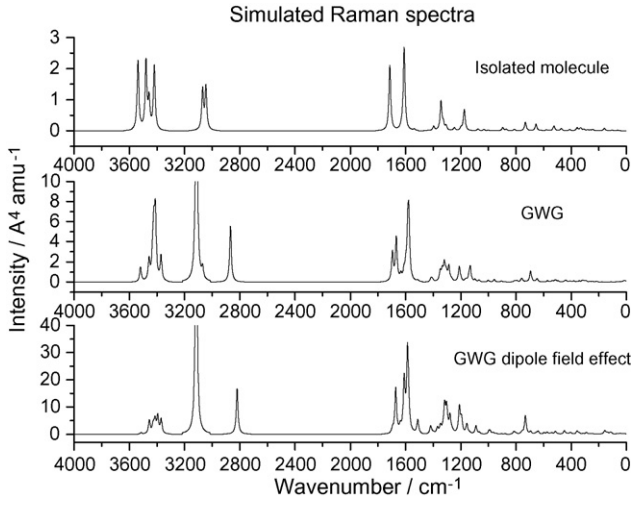

Fig. 10. Simulated Raman spectra of gallic acid.

chemical method overestimates the intensity of the CH stretch modes. Therefore these bands were truncated. The strong hydrogen bonds cause low frequency shifts in the GWG system as it is already observed in the IR spectra. It is in line with the general experience that the formation of hydrogen bonds increases the bond length of the O–H bond [45,46]. The less well-defined position of hydrogen atoms those are participating in hydrogen bonds cause the decrease of the height and the increase of the integrated intensity of hydroxyl stretch bands at around 3300 cm^{-1}.

4.7. Conclusions

The X-ray structure of the gallic acid crystal served a very good basis for applying the GWG molecular assembly to model the crystal structure for vibrational spectroscopic calculations of gallic acid. The effect of the chemical environment on the vibrational spectrum was investigated both experimentally and theoretically. In the first step, the addition of the crystalline water to gallic acid showed remarkable effect on its studied properties due to the very strong hydrogen bonds.

In the second stage, the solvent effect was modeled based Onsager's dipole field theory and it was found that the aqueous environment has essentially less significant effect on the vibrational spectra. In agreement with the results of X-ray measurements, geometry optimization shows that the interaction between two gallic acid and the water molecules are not symmetric in crystalline gallic acid. Thus the difference decreases between the two C–O bonds, while valence angles and dihedral angles also change in the vicinity of carboxylic acid moiety. In spite of this, aqueous environment acting as dipole field in the quantum chemical calculations has less significant effect on the GWG geometry. The inequality of the two gallic acid molecules is also discernible from the values of obtained atomic net charges and vibrational force constants.

The water of crystallization has very strong effect on gallic acid by increasing the number of the intermolecular hydrogen bonds significantly in the IR spectra. That is why the low frequency shifts of the OH stretch bands are observed. In the Raman spectra, some bands are broader in the spectrum of crystalline gallic acid than in that of the dry compound. The agreement between the experimental and simulated spectra is quite good.

Acknowledgements

The authors thank Prof. Gábor Keresztury for his help in this project and Prof. Allan Holmgren and Maine Ranheimer for their kind help in the experimental work. Mr. Csaba Kertész is also acknowledged for performing the single crystal X-ray diffraction measurement.

Appendix A. Supplementary data

Supplementary data associated with this article can be found, in the online version, at doi:10.1016/j.vibspec.2006.07.008.

References

[1] E. Sjöström, Wood Chemistry—Fundamentals and Applications, 2nd ed., Academic Press, San Diego, 1993.
[2] G. Svensson, Naturliga försvarssubstanser i trä—Litteraturstudie 1988, Trätek Institutet för Träteknisk Forskning, Stockholm, 1988(in Swedish).
[3] N.W.D.A. Eyles, T. Mitsunaga, R. Mihara, C. Mohammed, Forest Pathol. 34 (4) (2004) 225–232.
[4] A.R. Murray, S. Rodriguez, M.A. Frontera, M.A. Tomas, M.C. Mulet, Z. Naturforsch. C 59 (7–8) (2004) 477–480.
[5] J. Gonzalez, J.M. Cruz, H. Dominguez, J.C. Parajo, Food Chem. 84 (2) (2004) 243–251.
[6] V.R. Nsolomo, K. Venn, H. Solheim, Mycol. Res. 104 (2000) 1473–1479.
[7] K. Shimizu, R. Kondo, K. Sakai, J. Wood Sci. 48 (5) (2002) 446–450.
[8] P. Mammela, A. Tuomainen, H. Savolainen, J. Kangas, T. Vartiainen, L. Lindroos, J. Environ. Monit. 3 (5) (2001) 509–511.
[9] R.R. Madrera, D.B. Gomis, J.J.M. Alonso, J. Agric. Food Chem. 51 (27) (2003) 7969–7973.
[10] M. Murugananthan, G.B. Raju, S. Prabhakar, J. Chem. Technol. Biotechnol. 80 (10) (2005) 1188–1197.
[11] Z. Iqbal, S. Hiradate, A. Noda, S.I. Isojima, Y. Fujii, Weed Sci. 51 (5) (2003) 657–662.
[12] J. Ma, X.D. Luo, P. Protiva, H. Yang, C.Y. Ma, M.J. Basile, I.B. Weinstein, E.J. Kennelly, J. Nat. Prod. (7) (2003) 983–986.
[13] J. Kinjo, T. Nagao, T. Tanaka, G. Nonaka, M. Okawa, T. Nohara, H. Okabe, Biol. Pharm. Bull. 25 (9) (2002) 1238–1240.
[14] J. Singh, G.K. Rai, K. Upadhyay, R. Kumar, K.P. Singh, Ind. J. Agric. Sci. 74 (1) (2004) 3–5.
[15] C.D.V. Mendez, M.P. Forster, M.A. Rodriguez-Delgado, E.M. Rodriguez-Rodriguez, C.D. Romero, Eur. Food Res. Technol. 217 (4) (2003) 287–290.
[16] R.W. Owen, R. Haubner, W.E. Hull, G. Erben, B. Spiegelhalder, H. Bartsch, B. Haber, Food Chem. Toxicol. 41 (12) (2003) 1727–1738.
[17] O. Doka, D. Bicanic, Anal. Chem. 74 (9) (2002) 2157–2161.
[18] E. Giannakopoulos, K.C. Christoforidis, A. Tsipis, M. Jerzykiewicz, Y. Deligiannakis, J. Phys. Chem. A 109 (10) (2005) 2223–2232.
[19] A. Krilov, A. Holmgren, R. Gref, L.-O. Öhman, Holzforschung 47 (1993) 239–246.
[20] M. O'Coinceanainn, C. Astill, S. Schumm, Dalton Trans. (5) (2003) 801–807.
[21] J. Zolgharnein, H. Abdollahi, D. Jaefarifar, G.H. Azimi, Talanta 57 (6) (2002) 1067–1073.
[22] M.J. Hynes, M. O'Coinceanainn, J. Inorg. Biochem. 85 (2–3) (2001) 131–142.
[23] G. Keresztury, F. Billes, M. Kubinyi, T. Sundius, J. Phys. Chem. A 102 (1998) 1371–1380.
[24] M. Nonella, J. Phys. Chem. B 101 (1997) 1235–1246.
[25] M. Spoliti, L. Bencivenni, J.J. Quirante, F. Ramondo, J. Mol. Struct. Theochem. 390 (1997) 139–148.
[26] H.T. Flakus, M. Chełmecki, Spectrochim. Acta A 58 (2002) 179–196.
[27] I. Mohammed-Ziegler, F. Billes, J. Mol. Struct. Theochem. 618 (3) (2002) 259–265.
[28] S. Martinez, I. Stagljar, J. Mol. Struct. 640 (2003) 167–174.
[29] M. Leopoldini, T. Marino, N. Russo, M. Toscano, J. Phys. Chem. A 108 (22) (2004) 4916–4922.
[30] S.M. Fiuza, E. Van Besien, N. Milhazes, F. Borges, M.P.M. Marques, J. Mol. Struct. 693 (1–3) (2004) 103–118.
[31] C.A. Gomes, T.G. da Cruz, J.L. Andrade, N. Milhazes, F. Borges, M.P.M. Marques, J. Med. Chem. 46 (25) (2003) 5395–5401.
[32] C. Capelli, B. Mennucci, S. Monti, J. Phys. Chem. A 109 (2005) 1933–1943.
[33] P.J.A. Ribeiro-Claro, A.M. Amado, Spectrochim. Acta A 61 (2005) 2796–2797.
[34] K. Harms, XCAD4 Data Reduction Program for CAD4. Diffractometers, Philipps-Universität Marburg, Germany, 1996.
[35] G.M. Sheldrick, SHELXS-97 Program for Crystal Structure Solution, University of Göttingen, Germany, 1997.
[36] G.M. Sheldrick, SHELXL-97 Program for Crystal Structure Refinement, University of Göttingen, Germany, 1997.
[37] A.J.C. Wilson (Ed.), International Tables for X-ray Crystallography, vol. C, Kluwer Academic Publishers, Dordrecht, 1992, Tables 6.1.1.4 (pp. 500–502), 4.2.6.8 (pp. 219–222) and 4.2.4.2 (pp. 193–199).
[38] M.J. Frisch, G.W. Trucks, H.B. Schlegel, G.E. Scuseria, M.A. Robb, J.R. Cheeseman, J.A. Montgomery Jr., T. Vreven, K.N. Kudin, J.C. Burant, J.M. Millam, S.S. Iyengar, J. Tomasi, V. Barone, B. Mennucci, M. Cossi, G. Scalmani, N. Rega, G.A. Petersson, H. Nakatsuji, M. Hada, M. Ehara, K. Toyota, R. Fukuda, J. Hasegawa, M. Ishida, T. Nakajima, Y. Honda, O. Kitao, H. Nakai, M. Klene, X. Li, J.E. Knox, H.P. Hratchian, J.B. Cross, C. Adamo, J. Jaramillo, R. Gomperts, R.E. Stratmann, O. Yazyev, A.J. Austin, R. Cammi, C. Pomelli, J.W. Ochterski, P.Y. Ayala, K. Morokuma, G.A. Voth, P. Salvador, J.J. Dannenberg, V.G. Zakrzewski, S. Dapprich, A.D. Daniels, M.C. Strain, O. Farkas, D.K. Malick, A.D. Rabuck, K. Raghavachari, J.B. Foresman, J.V. Ortiz, Q. Cui, A.G. Baboul, S. Clifford, J. Cioslowski, B.B. Stefanov, G. Liu, A. Liashenko, P. Piskorz, I. Komaromi, R.L. Martin, D.J. Fox, T. Keith, M.A. Al-Laham, C.Y. Peng, A. Nanayakkara, M. Challacombe, P.M.W. Gill, B. Johnson, W. Chen, M.W. Wong, C. Gonzalez, J.A. Pople, Gaussian 03, Revision C. 02, Gaussian Inc., Wallingford, CT, 2004.
[39] R.W. Jiang, D.S. Ming, P.P.H. But, T.C.W. Mak, Acta Crystallogr. C 56 (2000) 594–595.
[40] N. Okabe, H. Kyoyama, M. Suzuki, Acta Crystallogr. E 57 (2001) o764–o766.
[41] A.L. Spek, J. Appl. Crystallogr. 36 (2003) 7–13.
[42] F.H. Allen, W.D.S. Motherwell, Acta Crystallogr. B 58 (2002) 407–422.
[43] J. Grell, J. Bernstein, G. Tinhofer, Acta Crystallogr. B 56 (2000) 1030–1043.
[44] L. Onsager, J. Am. Chem. Soc. 58 (1936) 1486–1493.
[45] D. Hadzi (Ed.), Theoretical Treatments of Hydrogen Bonding (Wiley Research Series in Theoretical Chemistry), Wiley, New York, 1997.
[46] P. Schuster, G. Zundel, C. Sandorfy, The Hydrogen Bond, North Holland, Amsterdam, 1976.